



Effect of 320-row CT reconstruction technology on fractional flow reserve derived from coronary CT angiography based on machine learning: single- versus multiple-cardiac periodic images

Ke Shi^{1#}, Feng-Feng Yang^{2#}, Nuo Si¹, Chen-Tao Zhu¹, Na Li¹, Xiao-Lin Dong¹, Yan Guo³, Tong Zhang¹

¹Department of Radiology, The Fourth Affiliated Hospital, Harbin Medical University, Harbin, China; ²Department of Radiology, The Second Hospital, Tianjin Medical University, Tianjin, China; ³GE Healthcare, Beijing, China

Contributions: (I) Conception and design: K Shi, FF Yang, Y Guo, T Zhang; (II) Administrative support: T Zhang; (III) Provision of study materials or patients: K Shi, FF Yang; (IV) Collection and assembly of data: K Shi, FF Yang; (V) Data analysis and interpretation: K Shi, FF Yang, Y Guo; (VI) Manuscript writing: All authors; (VII) Final approval of manuscript: All authors.

[#]These authors contributed equally to this work and should be considered as co-first authors.

Correspondence to: Prof. Tong Zhang. Department of Radiology, The Fourth Affiliated Hospital, Harbin Medical University, Harbin 150001, China. Email: yingxiang939@163.com.

Background: Fractional flow reserve derived from computed tomography (CT-FFR) can be used to noninvasively evaluate the functions of coronary arteries and has been widely welcomed in the field of cardiovascular research. However, whether different image reconstruction schemes have an effect on CT-FFR analysis through single- and multiple-cardiac periodic images in the same patient has not been investigated.

Methods: This study retrospectively enrolled 122 patients who underwent 320-row computed tomography (CT) examination with both single- and multiple-cardiac periodic reconstruction schemes; a total of 366 coronary arteries were analyzed. The lowest CT-FFR values of each vessel and the poststenosis CT-FFR values of the lesion-specific coronary artery were measured using the two reconstruction techniques. The Wilcoxon signed-rank test was used to compare differences in CT-FFR values between the two reconstruction techniques. Spearman correlation analysis was performed to determine the relationship between CT-FFR values derived using the two methods. Bland-Altman and intraclass correlation coefficient (ICC) analyses were performed to evaluate the consistency of CT-FFR values.

Results: In all blood vessels, the lowest CT-FFR values showed no significant differences between the two reconstruction techniques in the left anterior descending artery (LAD; $P=0.65$), left circumflex artery (LCx; $P=0.46$), or right coronary artery (RCA; $P=0.22$). In blood vessels with atherosclerotic plaques, the poststenosis CT-FFR values (2 cm distal to the maximum stenosis) exhibited no significant differences between the two reconstruction techniques in the LAD ($P=0.78$), LCx ($P=1.00$), or RCA ($P=1.00$). The mean CT-FFR values of single- and multiple-cardiac periodic images showed excellent correlation and minimal bias in all groups.

Conclusions: CT-FFR analysis based on an artificial intelligence deep learning neural network is stable and not affected by the type of 320-row CT reconstruction technology.

Keywords: Coronary artery disease (CAD); coronary computed tomography angiography (CCTA); fractional flow reserve (FFR); machine learning (ML)

Submitted Jun 24, 2021. Accepted for publication Mar 02, 2022.

doi: 10.21037/qims-21-659

View this article at: <https://dx.doi.org/10.21037/qims-21-659>

Introduction

Coronary artery disease (CAD) is an ischemic heart disease caused by atherosclerotic lesions in coronary arteries. It is one of the diseases with the highest morbidity and mortality in the world. CAD imposes a substantial burden on human health and social development. Therefore, early detection, accurate prediction, and timely intervention are particularly crucial (1). Fractional flow reserve (FFR) is the “gold standard” for evaluating the physiological function of coronary arteries. FFR-guided percutaneous coronary intervention (PCI) can improve the prognosis while reducing the medical costs of patients (2). However, the use of FFR in China is limited due to various factors, including its low penetration rate, invasive nature, high cost, lengthy operation time, lack of a standard fee structure, and inadequate medical insurance coverage (3,4).

In recent years, FFR derived from coronary computed tomography angiography (CCTA) has become widely used. CT based FFR was developed utilizing computed fluid dynamics (CFD) or, most recently, machine learning (ML). Many studies have reported that CT based FFR (FFR_{CT}, CT-FFR, FFRB) has a higher diagnostic accuracy than other non-invasive examination of heart disease under the reference of the gold standard invasive FFR (5-8). The first domestically approved CT-FFR product, which was developed and produced by Beijing Kunlun Medical Cloud Technology, has been officially used in clinical practice since January 2020. This coronary FFR calculation software (trade name: DEEPVESSEL FFR) is the world's first medical device based entirely on artificial intelligence deep learning neural networks. The device uses self-developed deep learning technology for blood vessel segmentation and reconstruction and FFR calculation, which significantly shortens the calculation time. Preliminary data have indicated that the use of this FFR calculation software in the planning of treatment decisions can improve the prognosis and quality of life of patients while reducing their medical costs while such advantages are rarely offered by imaging modalities (6).

Ideally, a complete data set of the entire heart anatomy should be acquired within a single phase of the cardiac cycle without patient movement (9). However, in reality, single cardiac periodic imaging can not be obtained in many cases due to an uncontrollable heart rate or scanning equipment limitations. Generally, if the heart rate exceeds 65 beats per minute, ectopic beats, arrhythmias, or electrocardiogram (ECG) artifacts occur, making it difficult to obtain single cardiac periodic images diagnostic quality. With some

early CT scanners, if the gantry rotation speed is not fast enough and the temporal resolution is insufficient, single cardiac cycle imaging will produce moving images, requiring continuous cardiac cycle images to be stitched together during postprocessing. Therefore, the different segments of the artery from the proximal to the distal end lack time consistency in terms of contrast turbidity (10). A segmented reconstruction technique that uses two or more segments from a continuous cardiac cycle for reconstruction can improve the time resolution; however, if changes in heart rate during the scan and spatial positions of heart subvolumes are not aligned, this technique can produce blur artifacts (9,11). However, it remains unclear whether the time unevenness of contrast medium delivery affects the functional diagnostic performance of CT-FFR. Therefore, the present study retrospectively analyzed CT-FFR values in the same patient through single- and multiple-cardiac periodic images to determine whether 320-row CT reconstruction technology affects CT-FFR values. We present the following article in accordance with the MDAR (Materials Design Analysis Reporting) checklist (available at <https://qims.amegroups.com/article/view/10.21037/qims-21-659/rc>).

Methods

Patient population

The study was conducted in accordance with the Declaration of Helsinki (as revised in 2013). This study was approved by the Medical Ethics Committee of The Fourth Affiliated Hospital, Harbin Medical University (No. 2021-LLSC-08). In this retrospective study, 266 patients who underwent CCTA according to clinical indications between December 25, 2020 and December 30, 2020 were included. All patients' informed consent for this retrospective study was waived. The exclusion criteria included the following: past myocardial infarction and capillary obstruction, severe arrhythmia, allergy to iodine contrast agent, pregnancy, unstable clinical symptoms, severe calcification, any coronary artery malformation (for example, coronary fistula, abnormal coronary origin, and abnormal coronary artery dilation), a history of coronary stent or bypass surgery, and severe image artifacts.

CT acquisition and image reconstruction

All CT examinations were performed using the Toshiba 320-row CT scanner (Aquilion ONE, Toshiba, Tokyo,

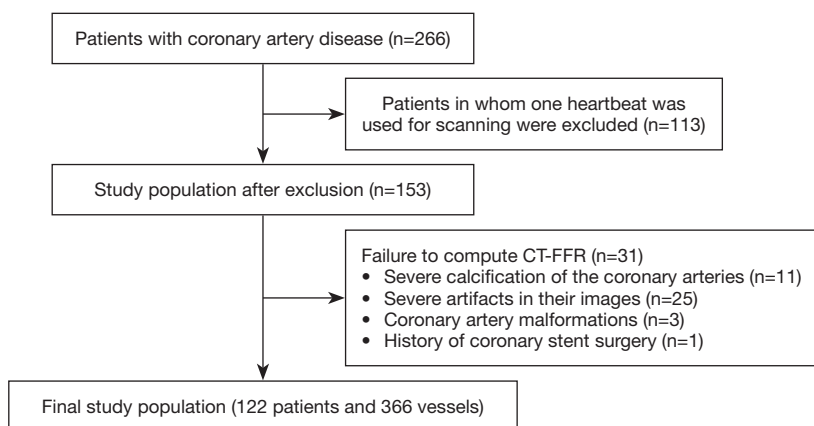


Figure 1 Flowchart of the study. CT-FFR, fractional flow reserve derived from computed tomography.

Japan). An indwelling 18-G trocar was placed in the antecubital vein using a dual-channel high-pressure syringe, and 40–70 mL of nonionic iodine contrast agent (iohexol injection containing 350 mg/L iodine, GE Healthcare, Beijing, China) was injected at a flow rate of 6 mL/s. The tube current was selected according to the patient's body mass index (BMI), and the tube voltage was set to 120 kV. The patient was asked to remain in the supine position and connected to the ECG monitor. The same monitoring scan layer was used at the ventricular level. We used a bolus tracking protocol for contrast medium injection, selected regions of interest for monitoring at the left ventricular level and initiated scanning manually when the left ventricle was observed to be brighter. The scanning range was 1.0 cm below the carina of the trachea to 1.5 cm at the lower edge of the heart. The patients received breath-holding training, and the number of heart beats required for scanning was determined according to the following scheme provided by the manufacturer: 1, 2, and 3 heartbeat scans for a heart rate of ≤ 65 , 66–79, and 80–99 beats/minute, respectively.

Because the aim of the study was to determine whether using single- or multiple-cardiac periodic images can affect CT-FFR analysis of the same patient, 113 patients for whom 1 heartbeat was used for scanning were excluded. To obtain the best phase of multicycle reconstruction (MCR) images, the best phase of the multiple heart-beat scan was selected for retrospective reconstruction. Then, secondary single-sector reconstruction of the MCR images was performed to obtain half-cycle reconstruction (HCR) images. The MCR images included two- and three-cycle reconstruction images. HCR images were reconstructed in adherence with the following steps. Firstly, selected the

cardiac cycle with a longer R-R interval through ECG editing. If the quality of the reconstructed image cannot meet the diagnostic requirements, selected another cardiac cycle to repeat the entire reconstruction step. The heart rate of the cardiac cycle with a longer R-R interval was slower, the velocity of the heart cavity wall was smaller, the duration of the optimal imaging phase was longer, and the coronary artery was less affected by respiratory motion and other factors, so the quality of the reconstructed image higher. Subsequently, the level of coronary artery display was selected and Cardio imageXact software was used to reconstruct all dynamic images of the cardiac cycle at this level. The best absolute time phase for coronary artery display was selected, and the complete image of the selected time phase was reconstructed with a reformat thickness of 0.5 mm and a reformat interval of 0.5 mm. The collected data were transferred to a Vitrea Fx workstation for postprocessing including multiplanar reformation (MPR), curved MPR, and volume reformation.

Image analysis

Image quality was evaluated using a four-point grading system comprising four levels: poor, medium, good, and excellent (12,13). Only images of good or excellent quality in both single- and multiple-cardiac periodic images were included. Images with severe calcifications and artifacts were deemed to be of substandard (poor and medium) quality, and could not be used for CT-FFR analysis. The numbers of CCTA images of poor, medium, good, and excellent quality were 1, 40, 60, 205, respectively. *Figure 1* shows a detailed timeline of the study protocol.

All CT images were analyzed by two experienced senior radiologists working separately. The results of CCTA were not affected by patients, scan order, or previous reports. For most CCTA reports and diagnoses, the two radiologists reached a consensus through negotiation. In the two cases of disagreement which arose, the final decision was made by a senior physician. The coronary artery tree was evaluated according to the 18-segment coronary artery segmentation system developed by the American Society of Cardiovascular Computed Tomography in 2014 (14), and the Coronary Artery Disease-Reporting and Data System (CAD-RADS) was used to visually assess the severity of stenosis in each segment (15). The degree of stenosis was graded as follows: 0, no stenosis; 1, slight stenosis (<25% stenosis); 2, mild stenosis (25–49% stenosis); 3, moderate stenosis (50–69% stenosis); 4, severe stenosis (70–99% stenosis); and 5, occlusion (100% stenosis). A stenosis diameter of $\geq 25\%$ was defined as a lesion-specific coronary artery.

CT-FFR analysis

CT-FFR analysis was performed using coronary FFR calculation software, which is a new generation of artificial intelligence technology developed and produced by Beijing Kunlun Medical Cloud Technology (16). All CCTA data were transmitted to the cloud workstation in the standard Digital Imaging and Communications in Medicine (DICOM) format. The CT-FFR core laboratory only had access to the CCTA dataset. The software is based on a supervised deep learning and neural net model which is trained in advance to map extracted three-dimensional (3D) vascular structures and the corresponding blood flow estimation (17). It fully considers the artery tree structure, lesion-specific information, spatial relationship and the influences of other branches for the blood flow dynamics. The result output time was 5–10 minutes per case, and the success rate of our CT-FFR analysis was 85%. The software provides a specific 3D model of the coronary artery, and the researcher can obtain the CT-FFR value at any given point along the length of the coronary artery. Following the reporting recommendation of CT-FFR (18) as well as the standardized SCCT guidelines (14), we further extracted poststenosis CT-FFR values or the lowest CT-FFR values from the major coronary arteries with lumen diameter of ≥ 1.8 mm only for the statistically analysis in this study. It should be noted that the artery was still considered as the major artery if its diameter decreased below 1.8 and then

recovered to ≥ 1.8 mm.

The lowest CT-FFR value of each vessel (the CT-FFR value at the distal end of the vessel) was recorded. If the CT-FFR value was ≤ 0.8 , the patient was diagnosed as having obstructive CAD. At the same time, the position of the lesion-specific coronary artery stenosis corresponded to that on the 3D coronary artery model, and the same ischemic threshold was used to record the poststenosis CT-FFR value of the lesion-specific coronary artery (the CT-FFR value at 2 cm distal to the lesion) (18–20). The lowest CT-FFR values were compared between all blood vessels, and the poststenosis CT-FFR values were compared between the lesion-specific coronary arteries. For each pair of CT-FFR values obtained using the two reconstruction techniques, the same position in the 3D anatomical model was selected for statistics.

Statistical analysis

All statistical analyses were performed using R software, version 3.6.2. All analyses were performed for each blood vessel. Continuous variables are expressed as the mean and standard deviation (SD), whereas categorical variables are expressed as frequency and percentage. The results of the Shapiro-Wilk test indicated that paired differences in the CT-FFR data set were not normally distributed. To evaluate the difference in CT-FFR values between the two reconstruction techniques, the Wilcoxon signed-rank test was performed for all collected indicators, namely the lowest CT-FFR value of each epicardial coronary artery and the poststenosis CT-FFR value of each lesion-specific coronary artery. $P < 0.05$ was considered to be statistically significant. Spearman correlation analysis was performed to determine the relationship between CT-FFR values derived from the two methods. Bland-Altman and intraclass correlation coefficient (ICC) analyses were performed to evaluate the consistency of the CT-FFR values.

Results

Patient population

Of 153 eligible patients, 31 were excluded due to having at least 1 CCTA image that could not be analyzed through CT-FFR. Of these 31 patients, 11 had severe calcification of coronary arteries, 25 had severe artifacts in their images, 3 had coronary artery malformations, and 1 had a history of coronary stent surgery. A total of 366 coronary arteries from

Table 1 Patient characteristics

Characteristics	Value
No. of patients	122
Age (years)	57.4±11.1
Male	63 (51.6)
BMI (kg/m ²)	24.7±2.2
Cardiac risk factors	
Diabetes	34 (27.9)
Hypertension	63 (51.6)
Hyperlipidemia	32 (26.2)
Smoking	21 (17.2)
Drinking	9 (7.4)
Obesity	10 (8.2)

Values are expressed as the mean ± SD or number (percentage). BMI, body mass index; SD, standard deviation.

the remaining 122 patients were included in the analysis.

Table 1 lists the demographic data of the included patients. The average age of the patients was 57.4±11.1 years, and 51.6% of patients were male.

CT-FFR analysis

No significant differences in the left anterior descending artery (LAD; $P=0.65$), left circumflex artery (LCx; $P=0.46$), or right coronary artery (RCA; $P=0.22$) were observed between the lowest CT-FFR values of single- and multiple-cardiac periodic images (Figure 2, Table 2). Lesion-specific coronary arteries defined by a diameter stenosis (DS) of $\geq 25\%$ was observed in 53 coronary arteries in 38 patients. Among them, the number of vessels with a stenosis degree of $\geq 75\%$, 50–75%, and 25–50% was 9, 10, and 34, respectively. In blood vessels with atherosclerotic plaques, the poststenosis CT-FFR values (2 cm distal to the maximum stenosis) showed no significant differences in the LAD ($P=0.78$), LCx ($P=1.00$), or RCA ($P=1.00$; Figure 3, Table 2) between the two reconstruction techniques.

The mean CT-FFR values of single- and multiple-cardiac periodic images showed excellent correlation and minimal bias in each group (Figures 4,5). The scatter plot derived from the Spearman correlation analysis showed a monotonic relationship and excellent correlation between the CT-FFR values for each group collected in single-

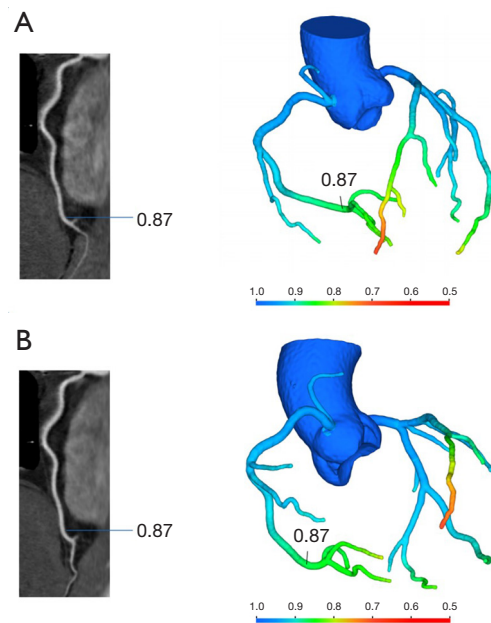


Figure 2 The normal RCA of a 45-year-old male patient. The CTA image and the corresponding CT-FFR model obtained from the patient using single- and multiple-cardiac periodic reconstruction technologies are shown. (A) Curved planar reconstruction and the corresponding CT-FFR model of single-cardiac periodic images. (B) Curved planar reconstruction and the corresponding CT-FFR model of multiple-cardiac periodic images. Examples of nadir CT-FFR values are marked in blue and black. RCA, right coronary artery; CTA, computed tomography angiography; CT-FFR, fractional flow reserve derived from computed tomography.

and multiple-cardiac periodic images (Table 3). Among all blood vessels, the lowest CT-FFR values in the LAD group ($r_s = 0.822$, $P < 0.001$; $ICC = 0.909$, $P < 0.001$) exhibited a very strong positive correlation. The lowest CT-FFR values in the LCx group ($r_s = 0.771$, $P < 0.001$; $ICC = 0.884$, $P < 0.001$) and the RCA group ($r_s = 0.797$, $P < 0.001$; $ICC = 0.899$, $P < 0.001$) showed a strong positive correlation. In blood vessels with atherosclerotic plaques, the poststenosis CT-FFR values in the LAD group ($r_s = 0.931$, $P < 0.001$; $ICC = 0.972$, $P < 0.001$), LCx group ($r_s = 0.975$, $P < 0.001$; $ICC = 0.982$, $P < 0.001$), and RCA group ($r_s = 0.820$, $P < 0.001$; $ICC = 0.978$, $P < 0.001$) all showed a very strong positive correlation. The results of Bland-Altman analysis revealed that the deviations between the lowest CT-FFR values of the LAD, LCx, and RCA, and between the poststenosis CT-FFR values of lesion-specific coronary arteries were

Table 2 Comparison of CT-FFR values

Vessel type	N	CT-FFR value (single-cardiac periodic)	CT-FFR value (multiple-cardiac periodic)	P value
Nadir/lowest CT-FFR values (all vessels)				
LAD	122	0.745 (0.052)	0.747 (0.050)	0.65
LCx	122	0.848 (0.052)	0.853 (0.051)	0.46
RCA	122	0.857 (0.035)	0.861 (0.037)	0.22
Poststenosis CT-FFR (vessels without plaques/CAD-RADS 0 excluded)				
LAD	29	0.813 (0.057)	0.809 (0.056)	0.78
LCx	10	0.856 (0.061)	0.859 (0.062)	1.00
RCA	14	0.846 (0.056)	0.845 (0.059)	1.00

Values are expressed as the mean (SD) and compared using the Wilcoxon signed-rank test. CT-FFR, fractional flow reserve derived from computed tomography; LAD, left anterior descending artery; LCx, left circumflex artery; RCA, right coronary artery; CAD-RADS, Coronary Artery Disease-Reporting and Data System; SD, standard deviation.

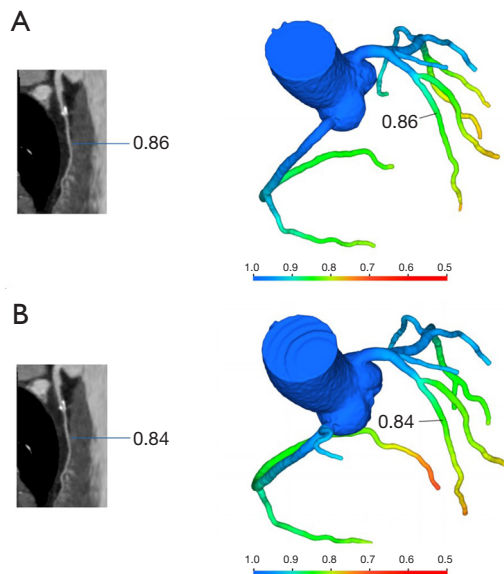


Figure 3 A 60-year-old female patient with mild stenosis of the proximal LAD lumen. The CTA image and the corresponding CT-FFR model obtained from the patient using single- and multiple-cardiac periodic reconstruction technologies. (A) Curved planar reconstruction and the corresponding CT-FFR model of single-cardiac periodic images. (B) Curved planar reconstruction and the corresponding CT-FFR model of multiple-cardiac periodic images. Examples of poststenosis CT-FFR values are marked in blue and black. LAD, left anterior descending artery; CTA, computed tomography angiography; CT-FFR, fractional flow reserve derived from computed tomography.

negligible (*Table 4*).

Discussion

The results of this study revealed that CT-FFR values were consistent between single- and multiple-cardiac periodic images, and that the reconstruction technology did not affect the functional evaluation ability of the heart. Compared with that of single cardiac periodic acquisition, multiple cardiac periodic acquisition had a smaller pitch and longer scan time. Therefore, the patient had to receive more radiation dose, and the collection efficiency would be greatly reduced. The radiation dose of multiple-cardiac periodic images in our study was 12.4 ± 5.3 mSv, while the true radiation dose of single-cardiac periodic images was only 5.0 ± 1.9 mSv. Interestingly, the results of this study suggest that CCTA can be performed at low radiation doses.

Theoretically, the principles of single cardiac periodic scanning images and HCR images generated by MCR images are the same; in both cases, the data used to reconstruct cross-sectional images are collected within a single cardiac cycle. HCR data based on post reconstruction can represent the real single heart beat scan. MCR images can be affected by heart rate fluctuations or poor breath-holding of patients, which results in inconsistent spatial positions of original data collected in the same phase. Moreover, changes in heart rate can affect the duration of the diastolic period and the degree of diastolic filling,

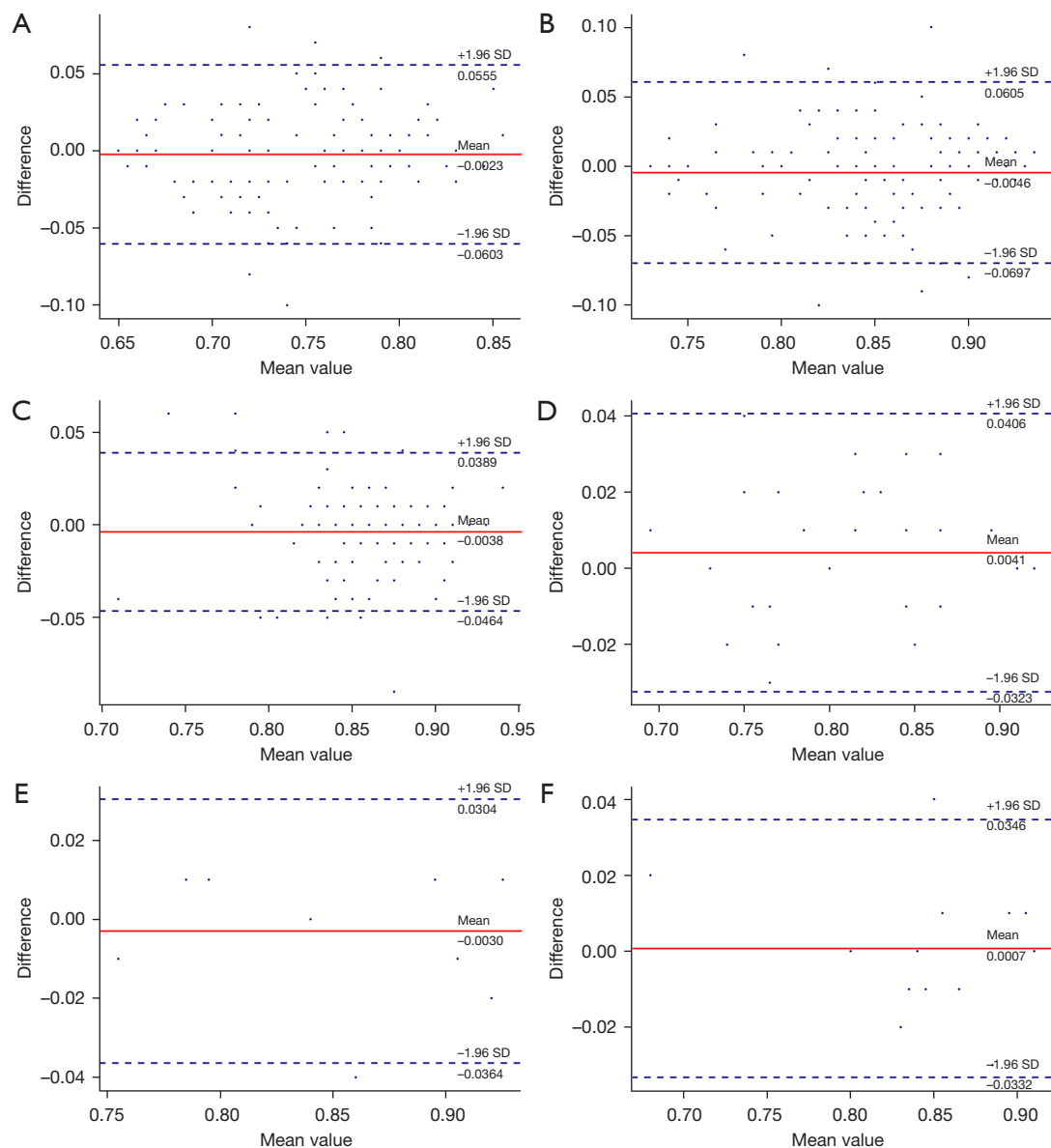


Figure 4 Bland-Altman analysis of CT-FFR values: single-cardiac periodic images versus multiple-cardiac periodic images. CT-FFR values of single- and multiple-cardiac periodic images show minimal bias. Nadir CT-FFR values for (A) LAD, (B) LCx, and (C) RCA, and poststenosis CT-FFR values for (D) LAD, (E) LCx, and (F) RCA. CT-FFR, fractional flow reserve derived from computed tomography; LAD, left anterior descending artery; LCx, left circumflex artery; RCA, right coronary artery.

causing the position of the coronary artery to change between the first and next cardiac cycle. Under this circumstance, blood vessels reconstructed using fusion data would show distortion artifacts. Compared with MCR images generated using multiple heartbeat scans, the images of the two only contain the information of one cardiac cycle, the image information is slightly lost. There is no

inconsistency of the original data caused by the fusion of multiple cardiac cycles, so motion artifacts are reduced. At the same time, the signal-to-noise ratio and the contrast-to-noise ratio, which representing the objective quality of an image, decrease slightly. Because motion artifacts are the main factor affecting image quality, the slight decrease in the objective quality of the image is negligible when the

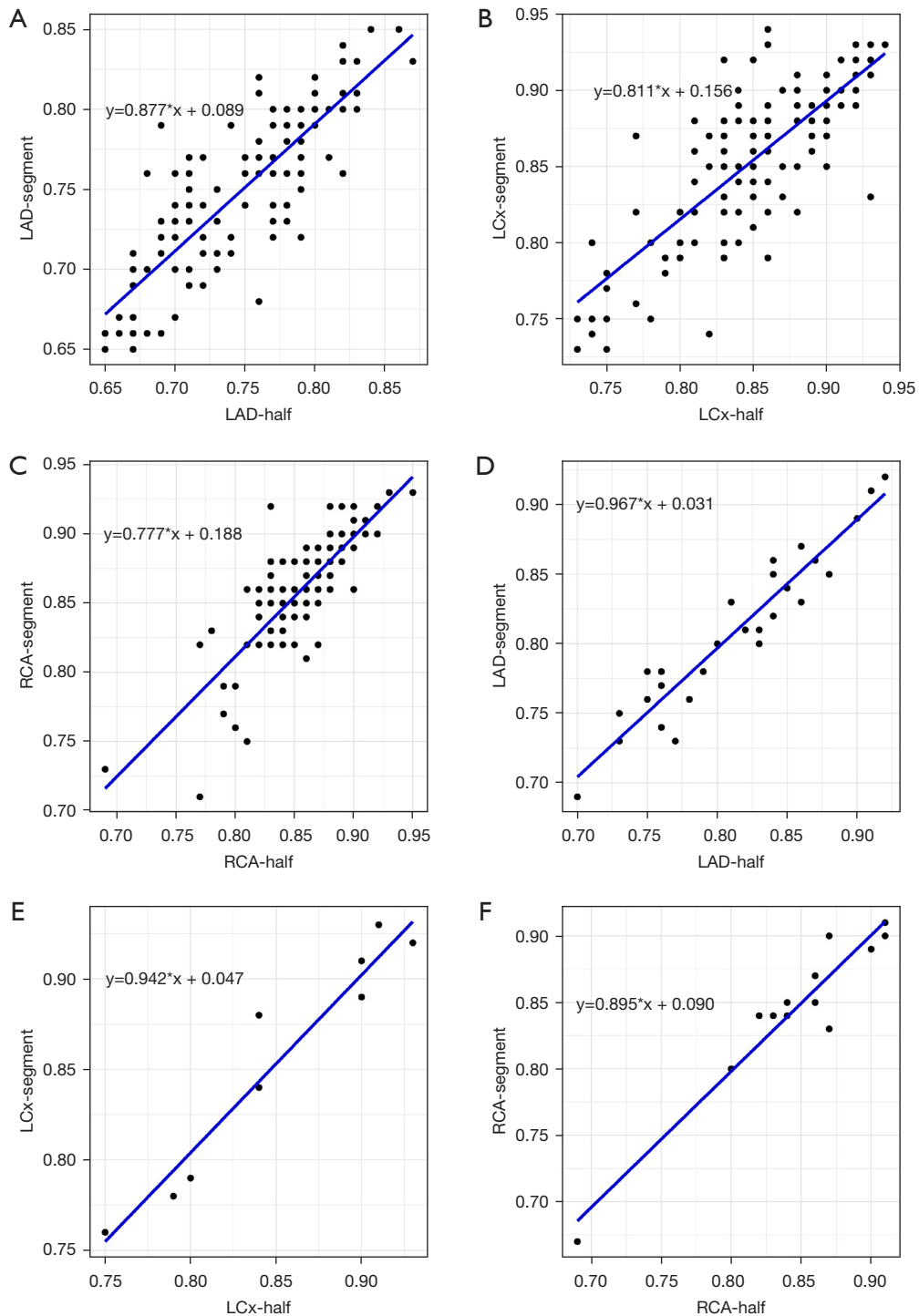


Figure 5 Scatter plot derived from Spearman correlation analysis of CT-FFR values: single-cardiac periodic images versus multiple-cardiac periodic images. CT-FFR values of single- and multiple-cardiac periodic images showed excellent correlation. Nadir CT-FFR values for (A) LAD, (B) LCx, and (C) RCA, and poststenosis CT-FFR values for (D) LAD, (E) LCx, and (F) RCA. LAD, left anterior descending artery; LCx, left circumflex artery; RCA, right coronary artery; CT-FFR, fractional flow reserve derived from computed tomography.

Table 3 Correlation and consistency analyses of the CT-FFR values

Vessel type	r_s	P value	ICC	P value
In all vessels				
LAD	0.822	<0.001*	0.909	<0.001*
LCx	0.771	<0.001*	0.884	<0.001*
RCA	0.797	<0.001*	0.899	<0.001*
In blood vessels with atherosclerotic plaques				
LAD	0.931	<0.001*	0.972	<0.001*
LCx	0.975	<0.001*	0.982	<0.001*
RCA	0.820	<0.001*	0.978	<0.001*

Values are derived from Spearman correlation analysis and ICC analysis. *, $P < 0.05$. CT-FFR, fractional flow reserve derived from computed tomography; ICC, intraclass correlation coefficient; LAD, left anterior descending artery; LCx, left circumflex artery; RCA, right coronary artery.

Table 4 Mean difference, SD and limits of agreement in Bland-Altman analysis

Variables	Nadir LAD	Nadir LCx	Nadir RCA	Lesion LAD	Lesion LCx	Lesion RCA
Mean difference	-0.0023	-0.0046	-0.0038	0.0041	-0.0030	0.0007
SD	0.0295	0.0332	0.0218	0.0186	0.0170	0.0173
Upper limit	0.0555	0.0605	0.0389	0.0406	0.0304	0.0346
Lower limit	-0.0603	-0.0697	-0.0464	-0.0323	-0.0364	-0.0332

Values are derived from Bland-Altman analyses. SD, standard deviation; LAD, left anterior descending artery; LCx, left circumflex artery; RCA, right coronary artery.

improvement in image distortion artifacts is considered. As discussed in previous literature, for patients with a heart rate of >65 beats/minute, HCR images have the best imaging quality for diagnosis (21). Xu *et al.* (22) conducted the first systematic evaluation of potential factors restricting the overall image quality of CT-FFR. The authors indicated that excellent image quality could improve the diagnostic performance of CT-FFR, facilitating improved detection of vessel-specific ischemia. This finding contradicts the results of our study, which found that different reconstruction techniques did not affect CT-FFR analysis. However, different reconstruction techniques can affect image quality. In future, relevant parameters that affect CT-FFR analysis need to be studied on a large scale.

As a new noninvasive assessment method for coronary artery restrictive stenosis, CT-FFR is efficient and widely used. This method can provide both anatomical and physiological information of the coronary artery and thus is widely applied in clinical practice. In recent years, researchers have attempted to identify factors that may affect CT-FFR analysis in order to improve its value and

increase its use in clinical practice. The absence of nitrate premedication can limit coronary luminal characterization, thus significantly affecting image quality and the accuracy of both anatomic and hemodynamic assessment using CCTA and CT-FFR analysis (23). Furthermore, Holmes *et al.* (24) showed that the dose of sublingual nitroglycerin did not affect CT-FFR analysis. Further, De Geer *et al.* (25) found that the diagnostic performance of CT-FFR did not differ between a tube voltage of 100 and 120 kVp; however, a tube voltage of 80 kVp improved the diagnostic performance. Jiang *et al.* (26) reported that the shape and severity of coronary artery calcification did not affect the diagnostic ability of CT-FFR in ischemia. Xu *et al.* (22) found that CCTA image quality and the patient's heart rate affected the diagnostic performance of CT-FFR, whereas sex, BMI, and calcification scores did not. Many factors can influence the diagnostic performance of CT-FFR, and because patient-related decision-making regarding further diagnostic workup or invasive assessment critically depends on the accuracy of CT-FFR values, the identification of these factors is of clinical relevance (27). To our knowledge,

few studies of this kind have compared the effects of two reconstruction technologies individually. We used two reconstruction methods, single- and multiple-cardiac periodic reconstruction schemes, for the same patient at the same time, thereby eliminating the interference of other factors to the greatest extent possible.

This study had some limitations that should be addressed. First, because this was a retrospective analysis, inherent selection bias might exist. Second, the results of this study are applicable to CT-FFR calculation software based on ML, and whether the findings can be extended to CT-FFR derived from other algorithms remains unclear. Third, 320-row CT scanners are extremely advanced scanners with better image quality. Unfortunately, most hospitals only have 64- or 128-row scanners, and the results of this study may not be applicable to other CT scanners. Fourth, in our study, only a small number of blood vessels had $DS \geq 25\%$, and it may be necessary to expand the sample size for in-depth research on the applicability of our findings to different patients. A stratified analysis of patients with different degrees of stenosis in a large sample is necessary to explore the generalizability of our conclusions. At present, our research group is collecting further data for verification in subsequent studies. Fifth, due to the lack of standard calcification scoring, stratified analysis could not be performed in this study. Patients with severe calcification were excluded, and whether this affected the results of the CT-FFR analysis needs further verification. Finally, although we analyzed the CT-FFR values of two reconstruction protocols in the same patient, this study still lacks validation of CT-FFR results by invasive FFR.

Conclusions

CT-FFR analysis based on an artificial intelligence deep learning neural network is stable and not affected by the type of 320-row CT reconstruction technology.

Acknowledgments

Funding: This work was supported by the Beijing Cihua Medical Development Foundation Project (Research on CT-assisted diagnosis of coronary heart disease based on artificial intelligence).

Footnote

Reporting Checklist: The authors have completed the MDAR

(Materials Design Analysis Reporting) checklist. Available at <https://qims.amegroups.com/article/view/10.21037/qims-21-659/rc>

Conflicts of Interest: All authors have completed the ICMJE uniform disclosure form (available at <https://qims.amegroups.com/article/view/10.21037/qims-21-659/coif>). YG is employed by GE Healthcare, the other authors have no conflicts of interest to declare.

Ethical Statement: The authors are accountable for all aspects of the work in ensuring that questions related to the accuracy or integrity of any part of the work are appropriately investigated and resolved. The study was conducted in accordance with the Declaration of Helsinki (as revised in 2013). This study was approved by the Medical Ethics Committee of The Fourth Affiliated Hospital, Harbin Medical University (No. 2021-LLSC-08). The requirement to obtain patients' informed consent was waived for this retrospective study.

Open Access Statement: This is an Open Access article distributed in accordance with the Creative Commons Attribution-NonCommercial-NoDerivs 4.0 International License (CC BY-NC-ND 4.0), which permits the non-commercial replication and distribution of the article with the strict proviso that no changes or edits are made and the original work is properly cited (including links to both the formal publication through the relevant DOI and the license). See: <https://creativecommons.org/licenses/by-nc-nd/4.0/>.

References

- Huang AL, Maggiore PL, Brown RA, Turaga M, Reid AB, Merkur J, Blanke P, Leipsic JA. CT-Derived Fractional Flow Reserve (FFRCT): From Gatekeeping to Roadmapping. *Can Assoc Radiol J* 2020;71:201-7.
- Zuo W, Zhang R, Yang M, Ji Z, He Y, Su Y, Qu Y, Tao Z, Ma G. Clinical prediction models of fractional flow reserve: an exploration of the current evidence and appraisal of model performance. *Quant Imaging Med Surg* 2021;11:2642-57.
- Lu G, Wang P, Jin Z. Application of CT derived fractional flow reserve: Chinese expert recommendations. *Chin J Radiol* 2020;54:925-33.
- Xu L, Zhang L, Zhang J, Lyu B. Fractional flow reserve derived from CT: current status and future direction. *Chin J Radiol* 2020;54:921-4.

5. Coenen A, Kim YH, Kruk M, Tesche C, De Geer J, Kurata A, Lubbers ML, Daemen J, Itu L, Rapaka S, Sharma P, Schwemmer C, Persson A, Schoepf UJ, Kepka C, Hyun Yang D, Nieman K. Diagnostic Accuracy of a Machine-Learning Approach to Coronary Computed Tomographic Angiography-Based Fractional Flow Reserve: Result From the MACHINE Consortium. *Circ Cardiovasc Imaging* 2018;11:e007217.
6. Tesche C, De Cecco CN, Albrecht MH, Duguay TM, Bayer RR 2nd, Litwin SE, Steinberg DH, Schoepf UJ. Coronary CT Angiography-derived Fractional Flow Reserve. *Radiology* 2017;285:17-33.
7. Tesche C, De Cecco CN, Baumann S, Renker M, McLaurin TW, Duguay TM, Bayer RR 2nd, Steinberg DH, Grant KL, Canstein C, Schwemmer C, Schoebinger M, Itu LM, Rapaka S, Sharma P, Schoepf UJ. Coronary CT Angiography-derived Fractional Flow Reserve: Machine Learning Algorithm versus Computational Fluid Dynamics Modeling. *Radiology* 2018;288:64-72.
8. Zhang JM, Han H, Tan RS, Chai P, Fam JM, Teo L, et al. Diagnostic Performance of Fractional Flow Reserve From CT Coronary Angiography With Analytical Method. *Front Cardiovasc Med* 2021;8:739633.
9. Ohnesorge BM, Hofmann LK, Flohr TG, Schoepf UJ. CT for imaging coronary artery disease: defining the paradigm for its application. *Int J Cardiovasc Imaging* 2005;21:85-104.
10. Stuijzand WJ, Danad I, Raijmakers PG, Marcu CB, Heymans MW, van Kuijk CC, van Rossum AC, Nieman K, Min JK, Leipsic J, van Royen N, Knaapen P. Additional value of transluminal attenuation gradient in CT angiography to predict hemodynamic significance of coronary artery stenosis. *JACC Cardiovasc Imaging* 2014;7:374-86.
11. Steigner ML, Mitsouras D, Whitmore AG, Otero HJ, Wang C, Buckley O, Levit NA, Hussain AZ, Cai T, Mather RT, Smedby O, DiCarli MF, Rybicki FJ. Iodinated contrast opacification gradients in normal coronary arteries imaged with prospectively ECG-gated single heart beat 320-detector row computed tomography. *Circ Cardiovasc Imaging* 2010;3:179-86.
12. Yan C, Zhou G, Yang X, Lu X, Zeng M, Ji M. Image quality of automatic coronary CT angiography reconstruction for patients with HR ≥ 75 bpm using an AI-assisted 16-cm z-coverage CT scanner. *BMC Med Imaging* 2021;21:24.
13. Liang J, Sun Y, Ye Z, Sun Y, Xu L, Zhou Z, Thomsen B, Li J, Sun Z, Fan Z. Second-generation motion correction algorithm improves diagnostic accuracy of single-beat coronary CT angiography in patients with increased heart rate. *Eur Radiol* 2019;29:4215-27.
14. Leipsic J, Abbara S, Achenbach S, Cury R, Earls JP, Mancini GJ, Nieman K, Pontone G, Raff GL. SCCT guidelines for the interpretation and reporting of coronary CT angiography: a report of the Society of Cardiovascular Computed Tomography Guidelines Committee. *J Cardiovasc Comput Tomogr* 2014;8:342-58.
15. Cury RC, Abbara S, Achenbach S, Agatston A, Berman DS, Budoff MJ, Dill KE, Jacobs JE, Maroules CD, Rubin GD, Rybicki FJ, Schoepf UJ, Shaw LJ, Stillman AE, White CS, Woodard PK, Leipsic JA. CAD-RADS(TM) Coronary Artery Disease - Reporting and Data System. An expert consensus document of the Society of Cardiovascular Computed Tomography (SCCT), the American College of Radiology (ACR) and the North American Society for Cardiovascular Imaging (NASCI). Endorsed by the American College of Cardiology. *J Cardiovasc Comput Tomogr* 2016;10:269-81.
16. Liu X, Mo X, Zhang H, Yang G, Shi C, Hau WK. A 2-year investigation of the impact of the computed tomography-derived fractional flow reserve calculated using a deep learning algorithm on routine decision-making for coronary artery disease management. *Eur Radiol* 2021;31:7039-46.
17. Huang FY, Liu Q, Liu XX, Ma B, Zhu Y. Virtual fractional flow reserve and virtual coronary stent guided percutaneous coronary intervention. *Cardiol J* 2020;27:318-9.
18. Nørgaard BL, Fairbairn TA, Safian RD, Rabbat MG, Ko B, Jensen JM, Nieman K, Chinnaiyan KM, Sand NP, Matsuo H, Leipsic J, Raff G. Coronary CT Angiography-derived Fractional Flow Reserve Testing in Patients with Stable Coronary Artery Disease: Recommendations on Interpretation and Reporting. *Radiol Cardiothorac Imaging* 2019;1:e190050.
19. Rønnow Sand NP, Nissen L, Winther S, Petersen SE, Westra J, Christiansen EH, Larsen P, Holm NR, Isaksen C, Urbonaviciene G, Deibjerg L, Husain M, Thomsen KK, Rohold A, Bøtker HE, Böttcher M. Prediction of Coronary Revascularization in Stable Angina: Comparison of FFRCT With CMR Stress Perfusion Imaging. *JACC Cardiovasc Imaging* 2020;13:994-1004.
20. Omori H, Hara M, Sobue Y, Kawase Y, Mizukami T, Tanigaki T, Hirata T, Ota H, Okubo M, Hirakawa A, Suzuki T, Kondo T, Leipsic J, Nørgaard BL, Matsuo H. Determination of the Optimal Measurement Point

- for Fractional Flow Reserve Derived From CTA Using Pressure Wire Assessment as Reference. *AJR Am J Roentgenol* 2021;216:1492-9.
21. Tomizawa N, Yamamoto K, Akahane M, Torigoe R, Kiryu S, Ohtomo K. The feasibility of halfcycle reconstruction in high heart rates in coronary CT angiography using 320-row CT. *Int J Cardiovasc Imaging* 2013;29:907-11.
 22. Xu PP, Li JH, Zhou F, Jiang MD, Zhou CS, Lu MJ, et al. The influence of image quality on diagnostic performance of a machine learning-based fractional flow reserve derived from coronary CT angiography. *Eur Radiol* 2020;30:2525-34.
 23. Ihdahid AR, Ben Zekry S. Machine Learning CT FFR: The Evolving Role of On-Site Techniques. *Radiol Cardiothorac Imaging* 2020;2:e200228.
 24. Holmes KR, Fonte TA, Weir-McCall J, Anastasius M, Blanke P, Payne GW, Ellis J, Murphy DT, Taylor C, Leipsic JA, Sellers SL. Impact of sublingual nitroglycerin dosage on FFRCT assessment and coronary luminal volume-to-myocardial mass ratio. *Eur Radiol* 2019;29:6829-36.
 25. De Geer J, Coenen A, Kim YH, Kruk M, Tesche C, Schoepf UJ, Kepka C, Yang DH, Nieman K, Persson A. Effect of Tube Voltage on Diagnostic Performance of Fractional Flow Reserve Derived From Coronary CT Angiography With Machine Learning: Results From the MACHINE Registry. *AJR Am J Roentgenol* 2019;213:325-31.
 26. Di Jiang M, Zhang XL, Liu H, Tang CX, Li JH, Wang YN, et al. The effect of coronary calcification on diagnostic performance of machine learning-based CT-FFR: a Chinese multicenter study. *Eur Radiol* 2021;31:1482-93.
 27. Ammon F, Moshage M, Smolka S, Goeller M, Bittner DO, Achenbach S, Marwan M. Influence of reconstruction kernels on the accuracy of CT-derived fractional flow reserve. *Eur Radiol* 2022;32:2604-10.

Cite this article as: Shi K, Yang FF, Si N, Zhu CT, Li N, Dong XL, Guo Y, Zhang T. Effect of 320-row CT reconstruction technology on fractional flow reserve derived from coronary CT angiography based on machine learning: single- versus multiple-cardiac periodic images. *Quant Imaging Med Surg* 2022;12(6):3092-3103. doi: 10.21037/qims-21-659